



GE 214-269

GPO PRICE \$ _____

CFSTI PRICE(S) \$ _____

Hard copy (HC) 3.00

Microfiche (MF) 50

ff 653 July 65

STUDY OF THE GROWTH PARAMETERS INVOLVED IN SYNTHESIZING BORON CARBIDE FILAMENTS

by

A. Gatti, C. Mancuso, E. Feingold, R. Jakas

prepared for

NATIONAL AERONAUTICS AND SPACE ADMINISTRATION

CONTRACT NASw-1205

FACILITY FORM 608	N66 28634	(THRU)
	(ACCESSION NUMBER)	/
	53	(CODE)
	(PAGES)	00
	CR-75673	(CATEGORY)
	(NASA CR OR TMX OR AD NUMBER)	

SPACE SCIENCES LABORATORY

GENERAL ELECTRIC

MISSILE AND SPACE DIVISION

NOTICE

This report was prepared as an account of Government sponsored work. Neither the United States, nor the National Aeronautics and Space Administration (NASA), nor any person acting on behalf of NASA:

- A.) Makes any warranty or representation, expressed or implied, with respect to the accuracy, completeness, or usefulness of the information contained in this report, or that the use of any information, apparatus, method, or process disclosed in this report may not infringe privately owned rights; or
- B.) Assumes any liabilities with respect to the use of, or for damages resulting from the use of any information, apparatus, method or process disclosed in this report.

As used above, "person acting on behalf of NASA" includes any employee or contractor of NASA, or employee of such contractor, to the extent that such employee or contractor of NASA, or employee of such contractor prepares, disseminates, or provides access to, any information pursuant to his employment or contract with NASA, or his employment with such contractor.

Requests for copies of this report should be referred to

National Aeronautics and Space Administration
Office of Scientific and Technical Information
Attention: AFSS-A
Washington, D. C. 20546

214-269 (Final)

FINAL REPORT

STUDY OF THE GROWTH PARAMETERS INVOLVED
IN SYNTHESIZING BORON CARBIDE FILAMENTS

by

A. Gatti, C. Mancuso, E. Feingold, R. Jakas

prepared for

NATIONAL AERONAUTICS AND SPACE ADMINISTRATION

March 1, 1966

CONTRACT NASw-1205

Space Sciences Laboratory
GENERAL ELECTRIC COMPANY
Missile and Space Division

TABLE OF CONTENTS

<u>Section</u>	<u>Page</u>
I Introduction	1
II Experimental Procedures and Results	2
III Whisker Characterization	13
IV Composite Studies	27
V Conclusions	39
References	41
Acknowledgements	42

STUDY OF THE GROWTH PARAMETERS INVOLVED IN SYNTHESIZING BORON CARBIDE FILAMENTS

by A. Gatti, C. Mancuso, E. Feingold, and R. Jakas

General Electric Company

SUMMARY

The purpose of the present program has been the investigation of the following:

1. The growth of B_4C whiskers.
2. Characterization of the B_4C whiskers in terms of mechanical properties and crystalline perfection.
3. Incorporation of B_4C whiskers in composite specimens.

The B_4C whiskers were grown in a graphite resistance furnace. A new furnace was developed to provide a more desirable thermal gradient in the growth region. The results obtained by using this furnace were encouraging, and straight whiskers were produced. However, the current yield in the new furnace is lower than that of the previous growth furnace.

Calculations based on a theoretical growth mechanism indicate that the degree of supersaturation in the whisker growth zone of the new furnace is minimal and also explains the low whisker yield. It is anticipated that further adjustments of conditions in this zone should effectively enhance whisker growth.

Tensile tests were conducted on B_4C whiskers at room and elevated temperature. Two of the strongest specimens exhibited tensile strengths of 1×10^6 psi and 2×10^6 psi at room temperature. As would be expected, these whiskers also exhibited the highest degree of surface perfection, i.e., freedom from steps and overgrowths.

Elevated temperature tests of B_4C whiskers indicated that the whiskers suffer very little loss in strength up to $1000^\circ C$ to $1200^\circ C$. A sudden drop in strength beyond these temperatures is attributed to the oxidation of B_4C .

A study of the topography of a whisker which had a tested ultimate tensile strength of 2×10^6 psi revealed that whisker perfection dictates the ultimate strength of B_4C whiskers. Growth steps which are parallel to the whisker axis, $\langle h00 \rangle$, did not appear to seriously limit the tensile strength.

Composites of B_4C -aluminum were fabricated by hot pressing and liquid matrix infiltration techniques. Composite strength values were of the order of 20,000 psi.

STUDY OF THE GROWTH PARAMETERS INVOLVED
IN SYNTHESIZING BORON CARBIDE FILAMENTS

by

A. Gatti, C. Mancuso, E. Feingold, R. Jakas

ABSTRACT

Boron Carbide (B_4C) whiskers exhibit attractive properties for utilization in composite materials. In terms of their high strength, low density and high elastic modulus, these whiskers when utilized as reinforcements, offer great potential for high strength-to-weight or high stiffness-to-weight materials for future applications.

B_4C whiskers were grown by the vaporization at high temperature of B_4C powder and the subsequent condensation of this vapor in the form of whiskers at a lower temperature. Strength measurements were made on typical whisker specimens at both room and elevated temperatures. A room temperature tensile strength of 2×10^6 psi was measured for one such whisker. Characterization studies of B_4C whiskers by x-ray techniques, light microscopy techniques and electron microscopy techniques were made. Composites utilizing B_4C whiskers embedded in an aluminum matrix were fabricated by hot pressing and liquid infiltration methods and tested in tension at room and elevated temperatures.

I. INTRODUCTION

Boron Carbide (B_4C) whiskers exhibit attractive properties for utilization in composite materials. In terms of their high strength, low density and high elastic modulus, these whiskers when utilized as reinforcements, offer great potential for high strength-to-weight or high stiffness-to-weight materials for future applications. In addition, their refractory properties make them also valuable for high temperature applications.

Although more than one method of B_4C whisker growth has been studied, the most successful one to date has been the pure vapor method⁽¹⁾. This method consists of the vaporization of B_4C powder at high temperatures and subsequent condensation of B_4C whiskers on a graphite substrate at a lower temperature. It has been used to study the growth parameters and to obtain an adequate whisker supply for composite fabrication.

Tensile tests of B_4C whiskers were made to establish the actual strength values of the as-grown whiskers. The test results were also used to evaluate the growth process.

Characterization of B_4C whiskers is necessary to establish the nature of the whisker product. These studies of physical structure offer another method of product quality assessment.

Specimens which had been bend tested at room and elevated temperatures were studied. One of the purposes of this characterization is to establish whether the stronger whiskers are relatively free from surface imperfections.

II. EXPERIMENTAL PROCEDURES AND RESULTS

A. GROWTH STUDIES

Growth studies were performed in two different furnaces. One furnace has been used extensively in previous work⁽¹⁾, while the other furnace has been adapted to B_4C whisker growth, and will be described later. Also, growth studies were conducted on a process involving the B_2O_3/C reaction, which will also be discussed.

1. Growth of B_4C Whiskers by the "Pure Vapor Method"

Whiskers were grown successfully by the "pure vapor method" using a standard deposition mandrel and chimney which are shown in Figure 1. This mandrel and chimney were fitted into a furnace and were positioned over a fixture containing B_4C powder. The powder was vaporized at elevated temperatures, and the condensing the vapor species were deposited as B_4C whiskers on the mandrel and chimney which were located in a cooler position of the furnace. The whisker product was of good quality and of adequate quantity to supply whiskers for tensile testing and characterization studies.

The temperature gradient in the whisker growth zone was determined so that isothermal curves for the various levels of the growth chimney could be plotted. This was done by using a tungsten/tungsten-rhenium thermocouple mounted through a port in the top of the furnace. The temperature in the zone where the B_4C powder was vaporized was $1950^{\circ}C$, the temperature varied from $1855^{\circ}C$ in the hot portion of the chimney to $1725^{\circ}C$ in the cooler zone. The temperature gradient along the chimney length was approximately linear with distance.

2. Whisker Growth Experiments Using a Radial Furnace

A radial furnace was used to grow B_4C whiskers by the "pure vapor method" also. This furnace made it possible to provide a more uniform thermal gradient in the growth chamber, which also had a much greater surface area on which to nucleate and grow B_4C whiskers. The isotherms which influence whisker growth were non linear in the chimney-type furnace. In this new furnace, however, the thermal gradient extends in a radial direction, thus favoring the growth of straight B_4C whiskers. Since the isotherms are straight over larger distances, it was also hoped that longer whiskers could be grown.

The center tube of this furnace is heated by resistance, and has a twelve inch hot zone as shown in Figure 2. The outer graphite cylinders are used as radiation baffles, while the innermost one is used as the deposition mandrel for whisker growth. The center tube is slotted sym-

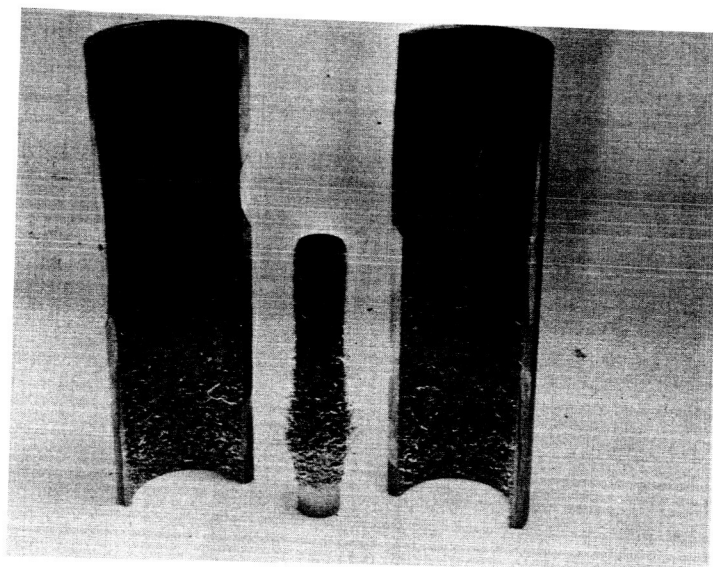


Figure 1. Photograph of Two Cut Sections of the Chimney and the Deposition Mandrel Showing Regions Where B_4C Whiskers Were Grown

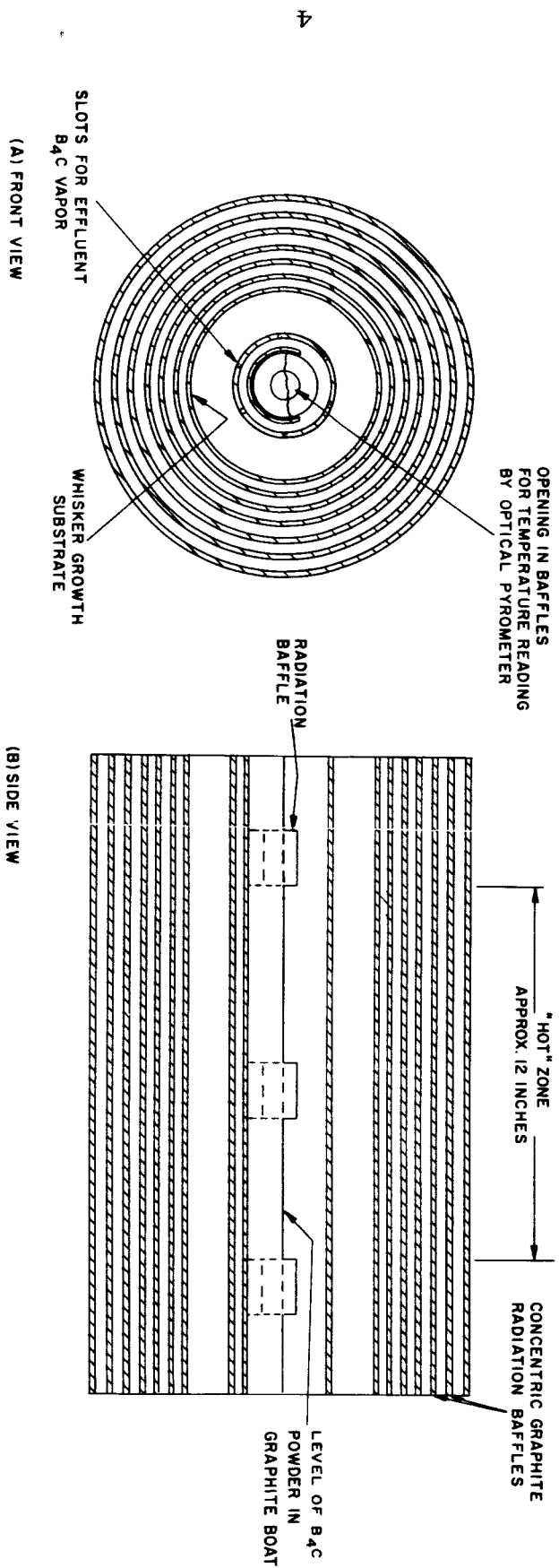


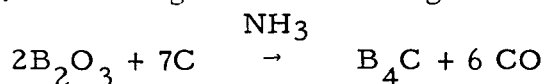
Figure 2. Radial Furnace

metrically in the hot zone and contains a graphite boat loaded with B₄C powder. The powder is evaporated and the resulting gaseous species pass through the slots and deposit as B₄C on the radiation baffle. There was a total of twelve removable radiation baffles arranged concentrically. By removing them one at a time in successive runs an adjustment of the surface temperature of the inner baffle was possible. By using various combinations of baffles B₄C whiskers were grown on the inside surface of the second baffle. A typical whisker product from this furnace is shown in Figure 3. The whiskers grown in this furnace were straight and not curved like those grown in the chimney furnace. These whiskers were the result of a 20-hour run, and the number of whiskers grown were much greater than in the chimney furnace, since available surface area was much larger.

The present growth rate is low and the largest whiskers were only 1 mm long. A subsequent 48 hour run produced whiskers which were only slightly larger than those shown in Figure 3. Whiskers were also grown in the end sections of the hot tube where the temperature gradients are similar to the chimney type furnace. During an extended run the whiskers grown in this region became quite long measuring about 1.2 cm and are shown in Figure 4. Results at this time are promising and warrant further experimentation with this furnace.

3. Growth of B₄C Whiskers Using the Boron Oxide and Carbon Reaction

Since reaction of SiO₂ with carbon in ammonia has been used to make SiC fibers⁽²⁾, an attempt was made to grow B₄C whiskers in a similar manner, according to the following reaction:



Several runs were made in the chimney furnace to try to make B₄C whiskers using boron oxide as a starting material.

Graphite powder was mixed with B₂O₃ powder in a graphite crucible. Ammonia gas was introduced and passed over the crucible. Deposits were formed in the chimney where the reaction zone temperature was 1400°C. There was no evidence of whisker like-growth in the deposit nor did chemical analysis show any B₄C formed. Hence, this method was not investigated further.

B. GROWTH MECHANISM OF B₄C WHISKERS

In 1955, G. W. Sears postulated a mechanism of whisker growth⁽³⁾ which will be used in the following discussion as a basis for providing an insight into the B₄C whisker growth environment. In a whisker growth process involving the evaporation of the pure substance into a gaseous



Figure 3. B_4C Whiskers Grown in the New Furnace. The Whiskers Were Scraped From the Graphite Deposition Baffle and Contain Small Lumps of Graphite. (Magnification 10X)



Figure 4. Photo at 6X of Whiskers Grown at End Sections of Radial Furnace

species of the same composition, the supersaturation ratio, α , is defined as:

$$\alpha = \frac{P}{P_0} \quad (1)$$

where P_0 is the vapor pressure of the gas at the temperature of the whisker surface and P is the actual pressure of the gas. According to Sears' postulation, the supersaturation in the vapor phase over a growing whisker may not exceed that value at which two-dimensional nucleation occurs. The relation between these parameters is given by:

$$\ln \alpha = \frac{\pi a \sigma^2 M}{\rho k R T^2 \ln B/N} \quad (2)$$

$$B = 10^{20} \text{ sec}^{-1}$$

a = is the interplaner spacing

σ = is the surface free energy

M = is the molecular weight of the vapor species

k = molecular gas constant

R = molar gas constant

T = absolute temperature

N = two dimensional nucleation rate

According to data obtained by H. E. Dobson and P. W. Gilles⁽⁴⁾, the vaporization of B_4C solid solutions was found to involve the preferential loss of boron, and that the mol fraction of boron in the vapor species is nearly 0.95. Thus, the use of Sears equation for $\ln \alpha$ was based on the molecular weight of boron, rather than that of B_4C .

Since the B_4C whiskers grow predominantly at the bottom of the chimney, the surface temperature was taken to be approximately 1880°C , and that of the vapor temperature to be 1920°C . The average of these two temperatures was used in the equation (1) to compute α , which was found to be:

$$\alpha \cong 1.32$$

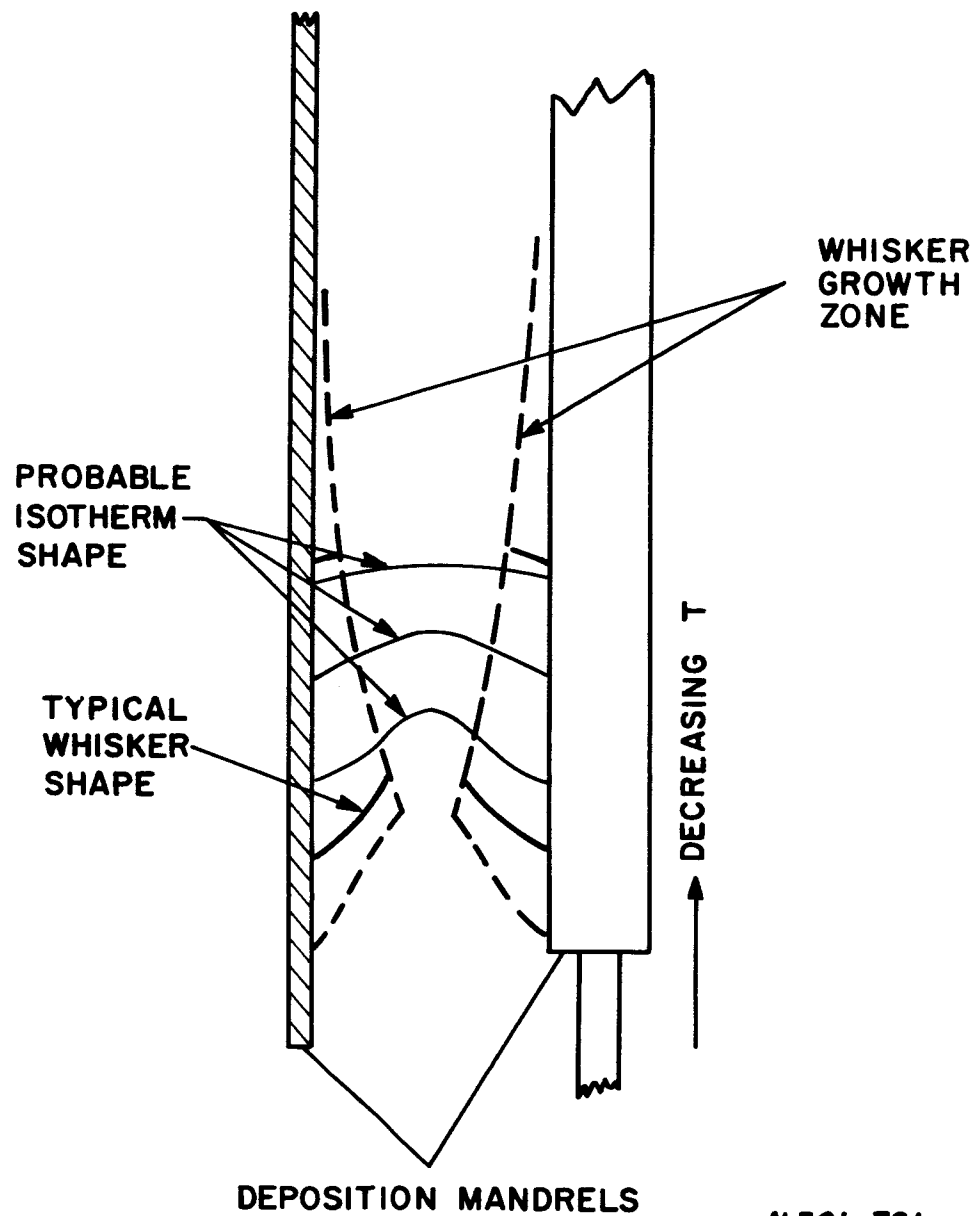
If a two dimensional nucleation rate of $1 \text{ sec}^{-1} \text{ cm}^{-2}$ is assumed as a measurable nucleation rate, the critical ratio (α_c) below which whisker growth should occur can be calculated from equation (2).

$$\begin{aligned} \text{If } B &= 10^{20} \text{ sec}^{-1} \\ a &= 5.61 \times 10^{-8} \text{ cm} \\ \sigma &\cong 1000 \text{ erg cm}^{-2} \\ M &= 10.81 \\ k &= 1.380 \times 10^{-16} \text{ erg deg}^{-1} \\ R &= 8.314 \times 10^7 \text{ erg mol}^{-1} \text{ deg}^{-1} \\ T &= 2063^\circ \text{K} \\ \text{then } \alpha_c &\cong 1.40 \end{aligned}$$

Considering the uncertainty of the value of σ , the surface free energy, the results indicate that the supersaturation is close to the value predicted for α_c . It is possible that some improvement in the supersaturation ratio can be made to further enhance whisker production in the chimney furnace. The existence of the non-linear thermal gradients are the most likely cause of the curved whisker growth.

Many features of B_4C whisker growth have been recognized from temperature gradients studies, optical microscopy, electron microscopy, electron diffraction and x-ray diffraction studies. The discussion which follows is based on knowledge based on these results.

Figure 5 is a schematic representation of the growth region as it appears during a typical run. It is to be noted that the largest whiskers appear first and a gradual decrease in length occurs as the distance away from the vapor source increases. It is postulated then that this distribution of size occurs by a mechanism which will now be described. Figure 6a shows a theoretical plot of both supersaturation and concentration as a function of temperature (or increasing distance) along the deposition mandrel. As is shown in Figure 6a, the supersaturation increases with decreasing temperature (or increasing distance) while the concentration decreases because the whiskers form a sink for B_4C vapor, thereby decreasing the amount of available vapor as a function of distance from the vapor source. Thus, Figure 6b shows the most probable representation of the supersaturation in the real system. This curve represents the supersaturation available for whisker growth as a function of temperature (or distance) along the deposition surface. This curve essentially duplicates



N 301-721

Figure 5. Schematic Diagram of the Probable Isotherm Contours Within the Growth Region, the Typical Whisker Shapes, and the Outline of Whisker Volume.

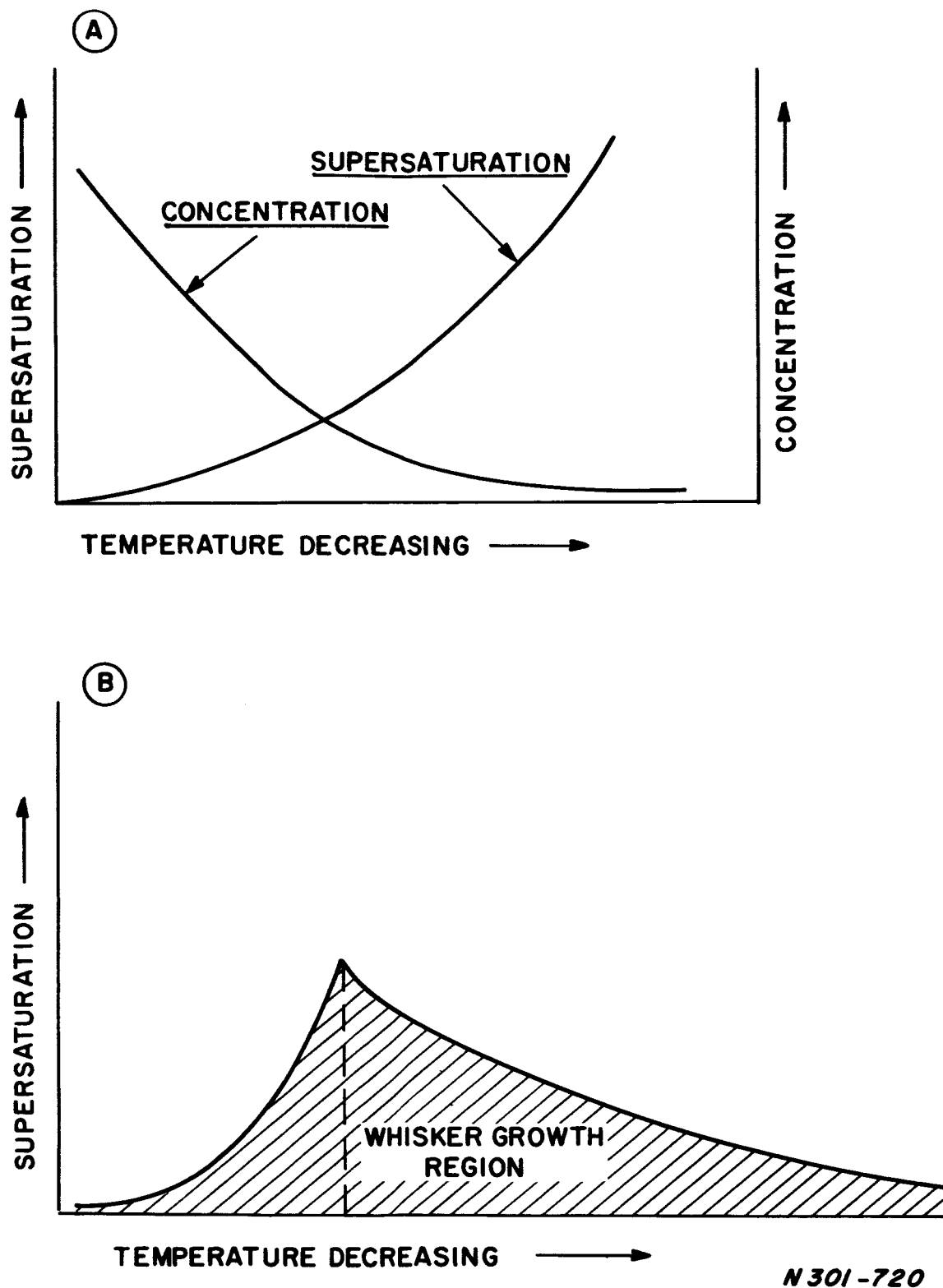


Figure 6. (A) Theoretical Plot of Both Supersaturation and Concentration as a Function of Temperature Within the Region of B_4C Whisker Growth. (B) Most Probable Representation of the Supersaturation in the Actual Growth Region.

the shape of the dotted curve shown in Figure 5, which represents the outline of whisker lengths grown as a function of temperature or distance during an actual whisker growth experiment. The high level of supersaturation in the area where whisker growth first begins can also explain the thickening of the whiskers with time.

Two further observations can also be explained by a further study of Figure 5. It has been observed that most B_4C whiskers are curved, and this curvature becomes less pronounced as the distance increases from the hot portion of the deposition zone. It is believed that this is due to temperature isotherms which are schematically drawn in Figure 5. Once nucleated, the whiskers appear to favor a constant supersaturation (constant temperature) for growth and faithfully follow the isotherm on which they begin to grow.

Whisker growth proceeds along unique crystallographic directions. Primary growth occurs in the \vec{a}_1 , or $\langle h00 \rangle$ direction. Secondary growth, which serves to widen the whisker into a blade, occurs in the \vec{a}_2 , or $\langle 0k0 \rangle$ direction. The thickness of the forming blade in the \vec{c} or $\langle 00l \rangle$ direction, remains relatively unchanged during its initial growth. The relative growth rates of length-to-width-to-thickness, during this period, are approximately 1:1/35:1/1500. These growth rates persist until the tip of the bladelet reaches a region of high supersaturation. Normal growth ceases when the tips of the longest approach the center of the growth volume. At this time in growth, a flag-like growth occurs on the whisker tips⁽⁶⁾. It is postulated that these flags arise from two sources. First, because of the extreme curvature of the initial isotherms and the gradual flattening of the isotherms further up the deposition tube a compression of the isotherms must take place in the center portion of the deposition volume (see Figure 5) leading to a high concentration of vapor in this region, and secondly because of the higher vapor concentration in this center region. The vapor concentration is higher, since there are no whiskers to act as sinks, in this region.

After a flag starts to grow, growth along the major whisker axis stops. From this time on, the major growth rate is in the \vec{c} or $\langle 00l \rangle$ direction, and the blade becomes thicker. The stacking fault configuration influences the surface character or topography of the whisker and characteristic topographical features result.

Although the above description of whisker growth is qualitative, it is consistent with the observations which have been made on B_4C whiskers in various stages of their development.

III. WHISKER CHARACTERIZATION

A. MECHANICAL PROPERTIES











Additional results have been obtained on the room temperature tensile properties of B_4C whiskers. These results, together with those previously reported⁽¹⁾, are shown in Figure 7. The new data are also shown in Table I. As previously explained⁽¹⁾, the value of the apparent elastic modulus, E^* , is low because of extraneous deflection of the grips. This value of E^* was not used in the computation of the fracture stress, which was obtained from direct measurement of the fracture area.

An examination of the data in Figure 7 indicates that there is little if any dependence of strength on cross-sectional area. Usually, it would be expected that the strength would increase with decreasing whisker size. The reason for this increase in strength is the decreasing probability of finding strength reducing flaws as the crystal size becomes smaller. However, optical examination of the surface of nearly all of B_4C whiskers indicates that sharp growth steps exist on their surfaces, which are similar to those shown previously⁽⁶⁾. The stress concentration effect of such growth steps has been studied by Marsh⁽⁷⁾, whose experimental data are shown in Figure 8. It may be seen that with sufficiently small values of r , the radius of curvature at the base of the step, the stress concentration factor approaches that of Griffith cracks. Marsh has measured values of r on growth steps of silicon whiskers, and has obtained a value of about 30\AA . Assuming this is typical of B_4C , it may be seen that large stress concentration factors may be obtained. Because there seems to be a systematic variation of ℓ , the step height, with size, it may be postulated that the growth steps in B_4C lead to a stress concentration factor of somewhere between 5 and 10, irrespective of the whisker size. This postulated effect of the growth steps is in accord with the data in Figure 7.

There are, however, exceptions. Specimens 6 and 7 (Table I) had strengths over 1.0×10^6 psi. The area of specimen 6, whose strength was 2.0×10^6 psi, was determined both by direct measurement and by replicating the fracture area in cellulose acetate and measuring the area of the replica optically. Close agreement was obtained between these two measurements, which makes the strength value fairly certain. It must be postulated, that if the Marsh analysis is applicable, the surface of this whisker should be comparatively smooth. The photographs of this particular whisker, (See Figure 11), indicate this conjecture is indeed true. These results also indicate that the direction to be followed in order to obtain high strength B_4C whiskers is to control the process parameters such that the growth steps are eliminated.

The high temperature properties of B_4C whiskers were determined in bending utilizing the apparatus previously described⁽⁶⁾. Some modifications were made, including the installation of a thermocouple adjacent to

TABLE I. STRENGTH OF B₄C WHISKERS

Spec. No.	Total Length mm	Gauge Length mm	Area, μ^2	E*, psi ⁽¹⁾	σ_u , psi	Cross-Section ⁽²⁾
1	---	0.78	12.3	39.8×10^6	398,000	
2	---	0.29	13.5	13.5	238,000	
3	0.53	0.35	4.30	52.2	718,000	
4	---	0.31	7.07	15.3	321,000	
5	---	0.44	68.4	19.2	240,000	
6	4.24	2.07	35.0	36.4	2,000,000	
7	2.48	0.42	46.8	24.2	1,225,000	
8	2.48	0.59	41.1	36.1	918,000	
9	Premature Break		---	23.2	654,000	
10	1.52	0.37	74.1	27.1	308,000	

{ Area checked
by both
replication and
direct obser-
vation.

(1) Apparent elastic modulus, See text.

(2) Fracture section observed on metallograph. Right angles on specimens 2, 3, and 4 may be 60°.

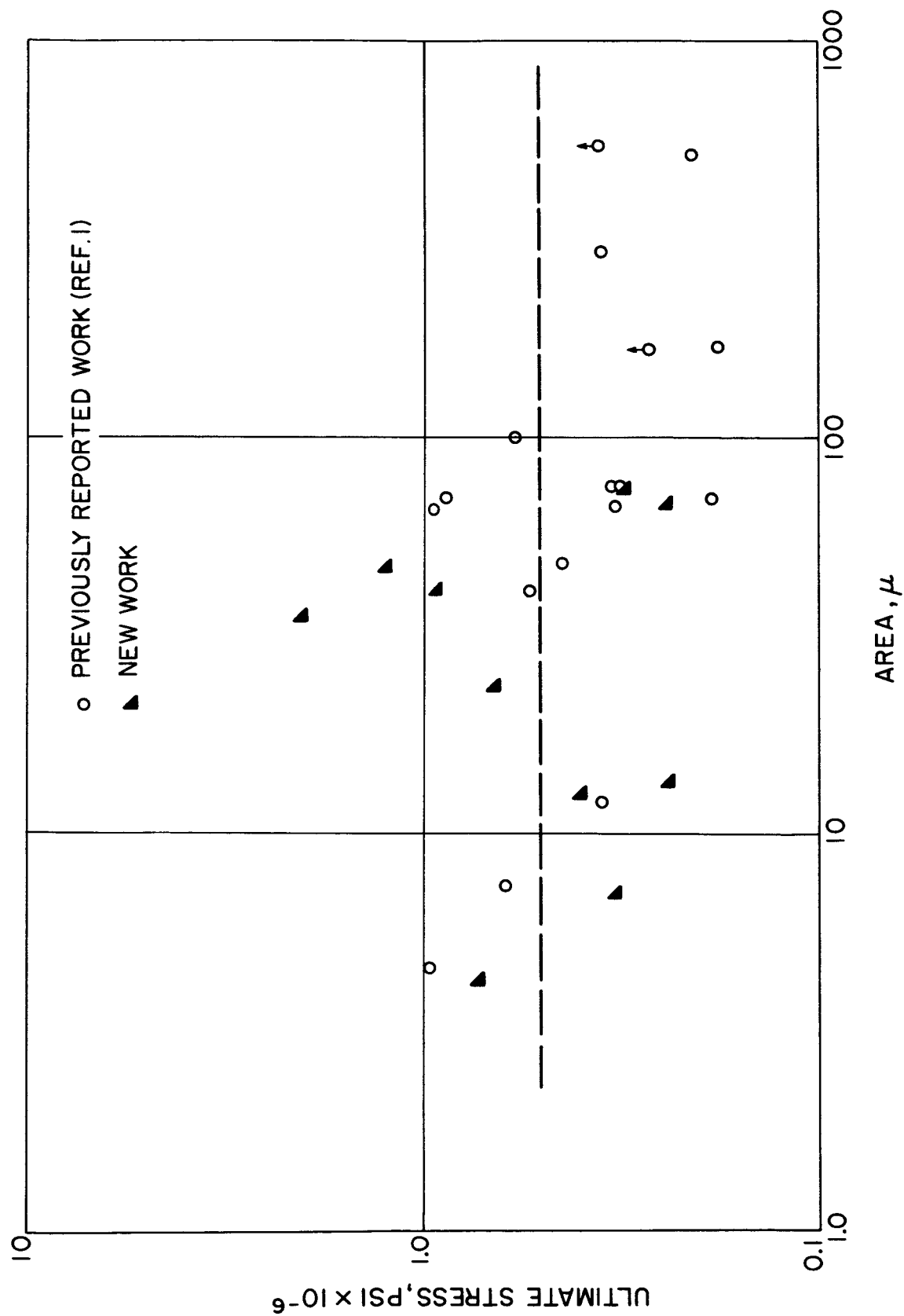


Figure 7. Room Temperature Tensile Strength of B_4C Whiskers

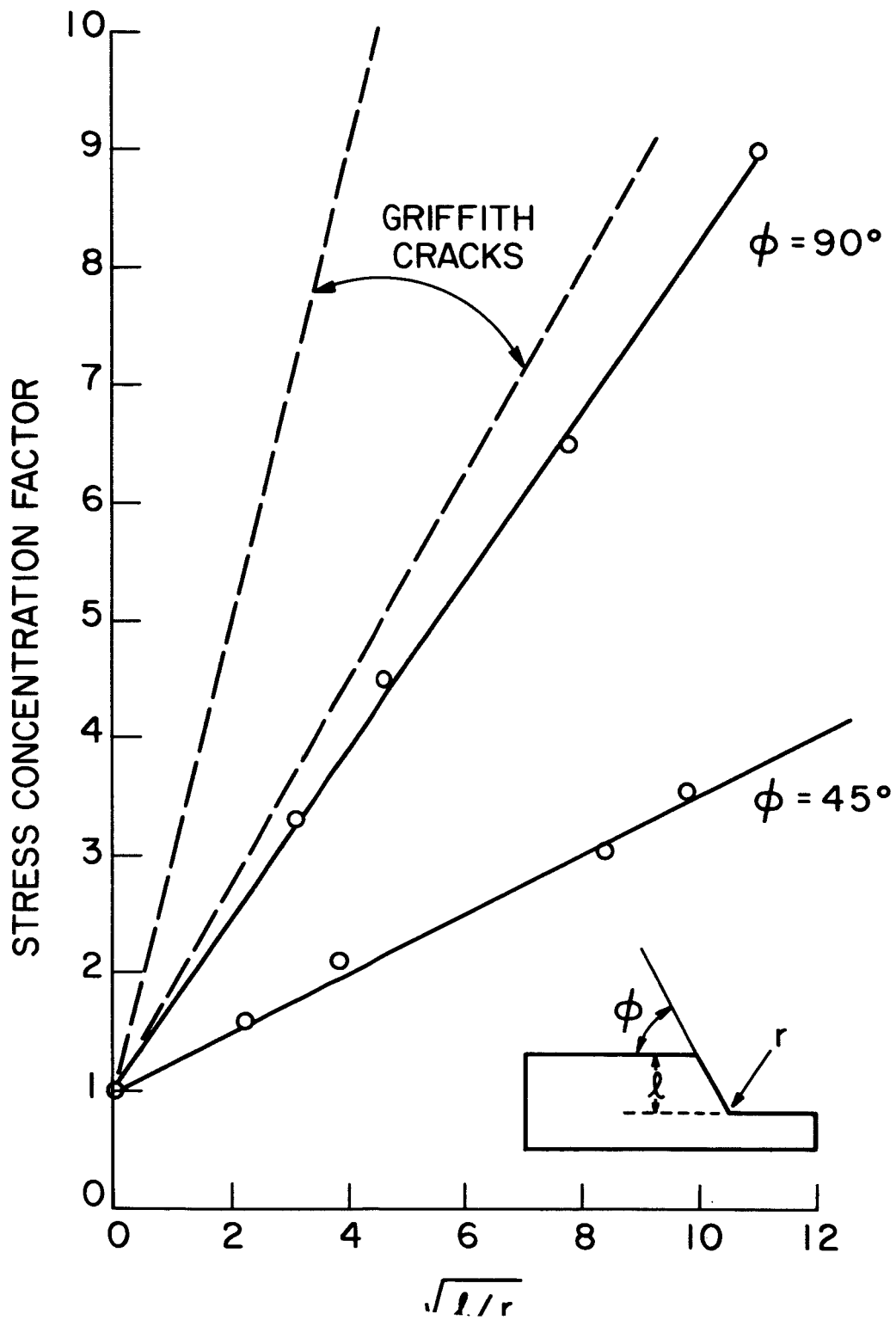


Figure 8. Stress Concentration Factor At Steps of Various Dimensions Compared With the Equivalent Crack Values. (After Marsh) ⁽⁷⁾

the specimen. The temperature as indicated by the thermocouple is about 5°C higher than the center (specimen) temperature as revealed by the direct comparison of two thermocouples. A schematic of the apparatus is shown in Figure 9.

In order to conduct the elevated temperature tests, relatively long B_4C whiskers having effective diameters of about 0.001" and having little apparent taper were selected. To obviate the necessity of measuring each cross-sectional area and to determine the spatial relation of the whisker with respect to the applied loads (necessary for moment of inertia measurements), a method was devised which allowed the hot strength to be determined as a fraction of the room temperature strength. The chosen whisker was fractured in bending at room temperature, and the fracture portions retrieved. These portions were then loaded to some fraction of the (average) room temperature breaking load, and the temperature was then increased until failure occurred. In this way the critical temperature for strength degradation, if any, was readily discernible.

The results are shown in Figure 10. The initial tests, performed in air, indicated very low strengths at moderate temperatures (about 700°C). This behavior was attributed to oxidation, so the balance of the tests were performed in a helium atmosphere. A plastic bag was suspended over the microfurnace and specimen assembly, and helium was allowed to flow in until the air was displaced. It is evident that this type of helium atmosphere contains residual oxygen.

Tests in helium indicated a sudden drop in strength between 1000°C and 1200°C . To make sure no silicon contamination from the quartz loading hooks was biasing the results, several tests were performed using a tungsten hook. No change in behavior was noted.

It is believed that the sudden strength decrease between 1000°C and 1200°C is due to oxidation resulting from residual oxygen in the system. Nazarchuk and Mekhanoshina⁽⁸⁾ have shown that at about 1100°C there is a sudden increase in the volatility of B_2O_3 , which is assumed to act as a protective film at lower temperature. This phenomena coincides with a sharp increase in the oxidation of B_4C . If sufficiently rapid oxidation occurs, the bending stress could decrease by either loss in cross-sectional area or by oxygen diffusion in the bulk B_4C .

B_4C whiskers which had been subjected to bend tests at elevated temperatures in various atmospheres were studied. A representative sampling of treated and characterized specimens are identified in Table II and are discussed below.

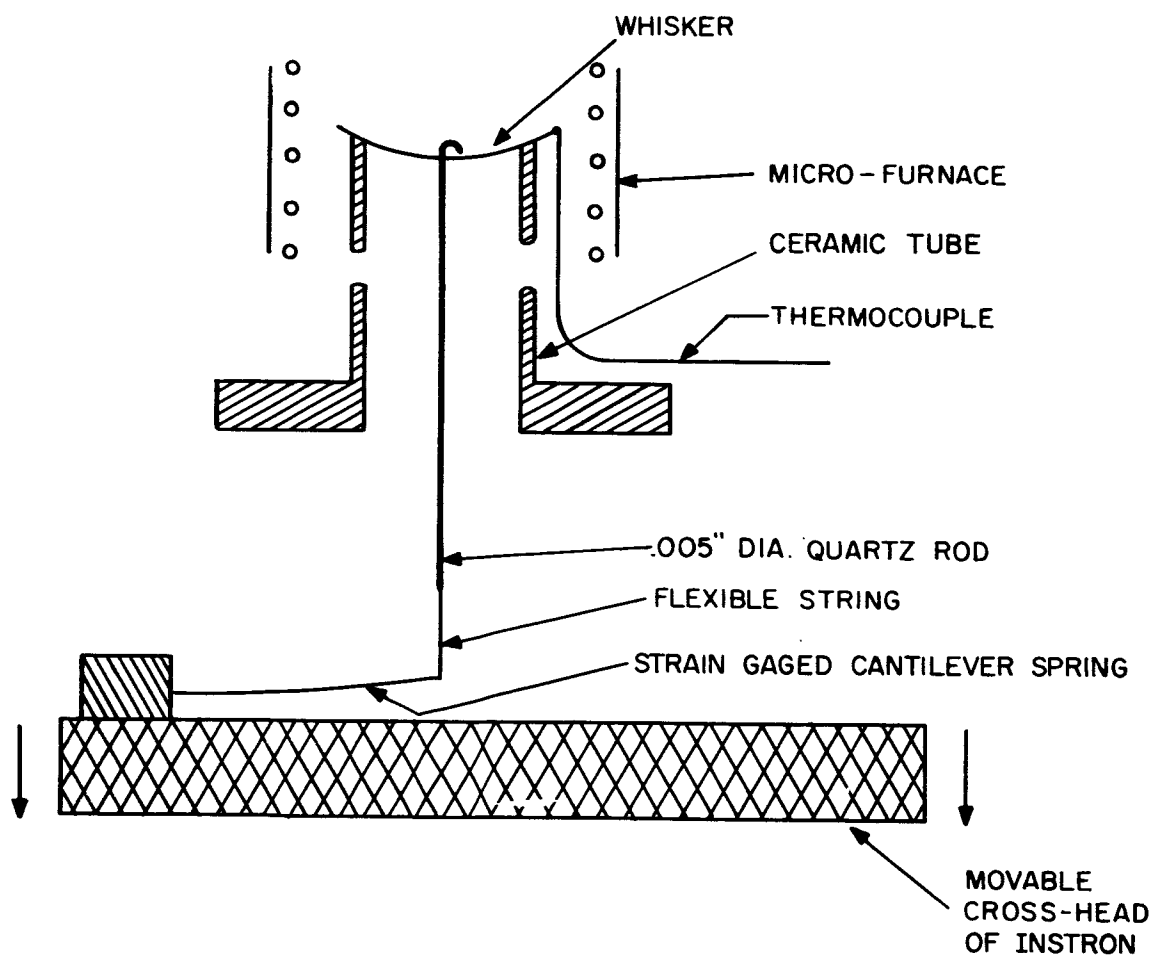


Figure 9. Apparatus for Flexure Testing Whiskers at Elevated Temperatures.

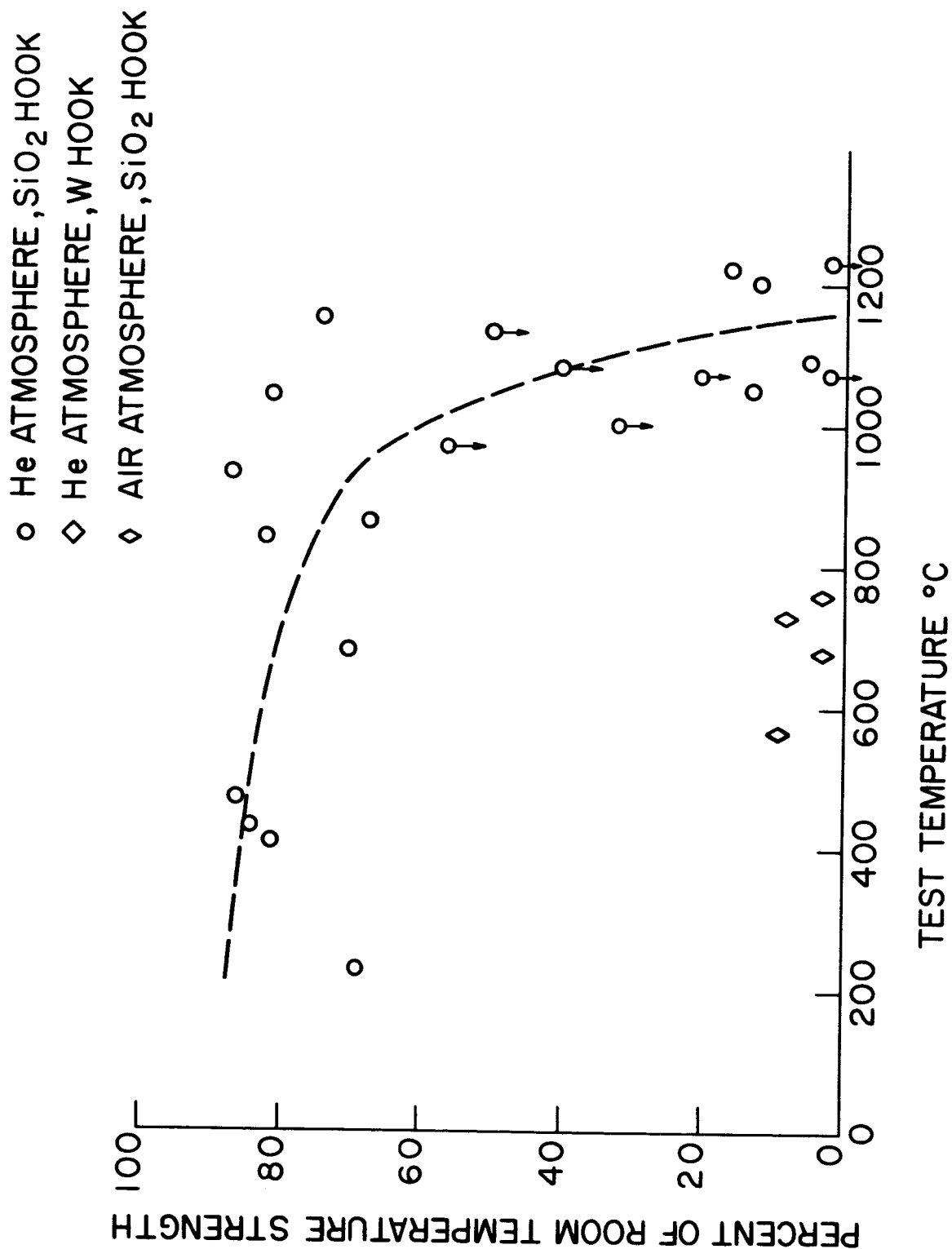


Figure 10. Hot Bend Strength of B₄C Whiskers

TABLE II
Thermally Treated and Characterized Specimens
Thermal Treatment

Spec. No.	Air	Helium	Temp°C	% Room Temp. Strength
6*	X		R. T.	100, (2×10^6 psi)
2	X		649	5
18	X		R. T.	100
4		X	1096	5
9		X	414	81
7		X	466	86
26		X	972	57
8		X	1045	81
10		X	1111	16
007	X		649	5

*Specimen 6 had been tension tested while the remaining specimens had been bend tested (3 point loading).

B. OPTICAL MICROSCOPY

The high tensile strength whisker specimen (No. 6 in Table II) was 2×10^6 psi, and was first examined with the optical microscope. Over the entire length of the retrieved fragment, ca. 2 mm, the whisker was found to be smoother than any other whisker thus far examined. Optical photomicrographs (magnification = 1220X) of this whisker are shown in Figure 11. This whisker was generally rectangular in cross section, ca. $2.5\mu \times 14\mu = 35\mu^2$. This area compares well with that measured in Section III, A. Figure 11A (oblique illumination) depicts one of the wide surfaces (filament width) near the fractured end. Figure 11B shows a narrow surface (filament thickness) at the same fractured end of the whisker. Figure 11C is the same field as Figure 11A made using polarized light. Several interesting features may be observed in these photographs.

With the exceptions of flutes, which are observed to run parallel to the whisker axis, the whisker is seen to be void of surface detail (note: the small light scattering detail which may be visible in Figure 11A is surface

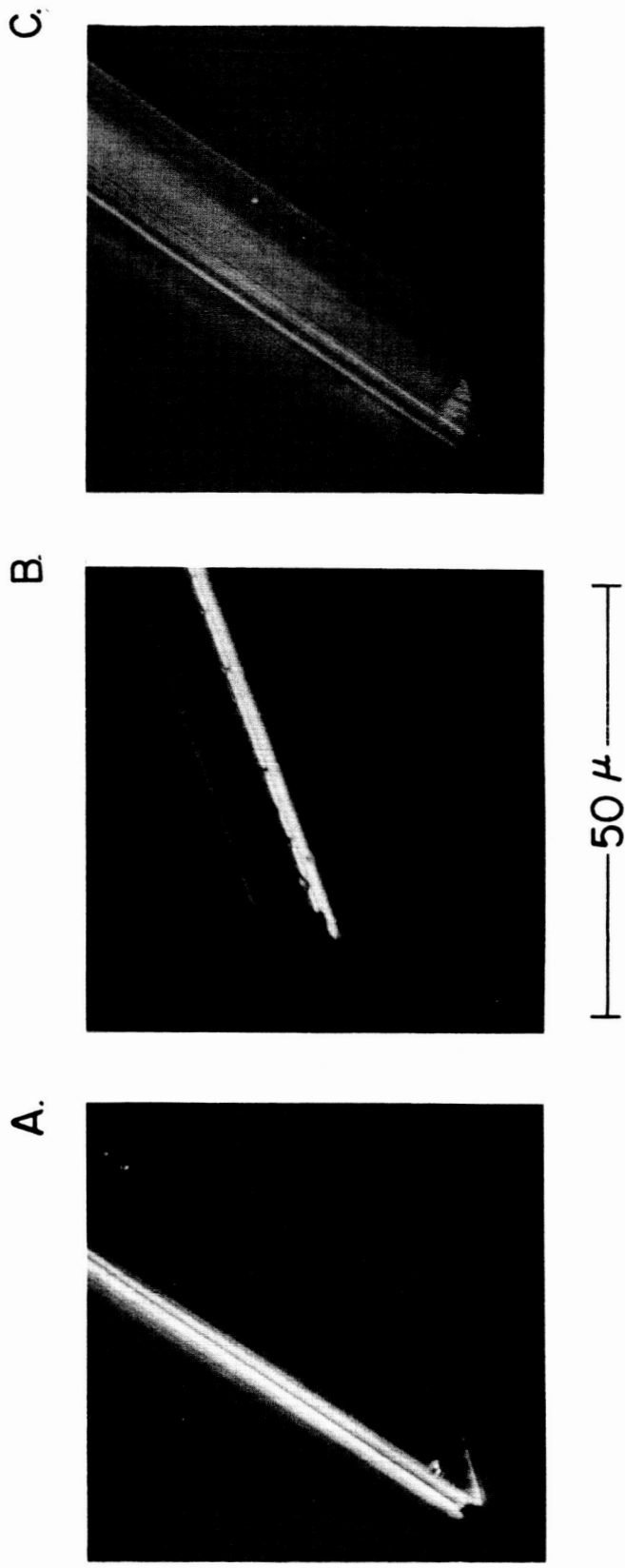


Figure 11. The Surface of a Strong B₄C Whisker, 2×10^6 psi (magnification = 1200X). A and C are of the Top Surface, B is of an Edge. C was Made Using Polarized Light.

dust, compare with 11C). Nowhere on this surface were there found to be steps of the type described in earlier reports^(1, 6). The edge of the whisker did, however, exhibit imperfections in the form of notches, (Figure 11B). These notch configurations may indeed have limited the ultimate tensile strength to only 2×10^6 psi. The detail visible on the fractured tip of the whisker in Figure 11C was discernible only through careful adjustment of the polarized light. This area may represent a twinned region. X-ray diffraction examination of the tip of this whisker tends to indicate that this a-type filament is twinned. Since it was found to be of the a-type, as incidently were all the whiskers examined during this period, the twin boundary on this whisker considering its direction as is shown in Figure 11C is the $(\bar{1}20)$ crystallographic plane.

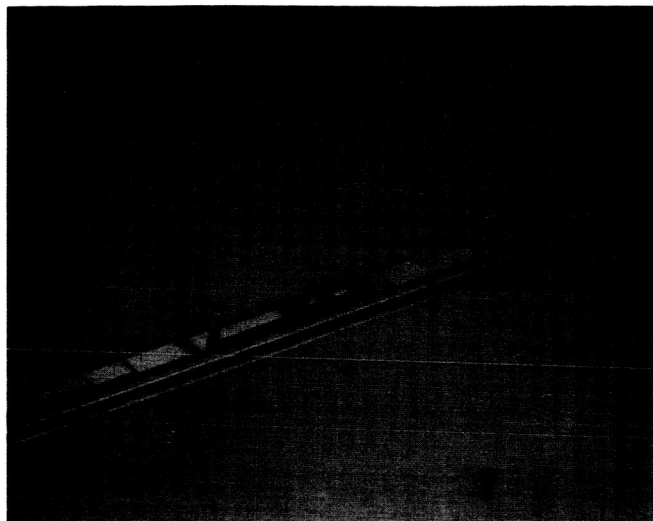
The remainder of the whiskers examined had surface details of the types previously reported^(1, 6). Additional examples of typical B_4C whisker surfaces are shown in the optical photomicrographs of Figure 12.

C. X-RAY DIFFRACTION

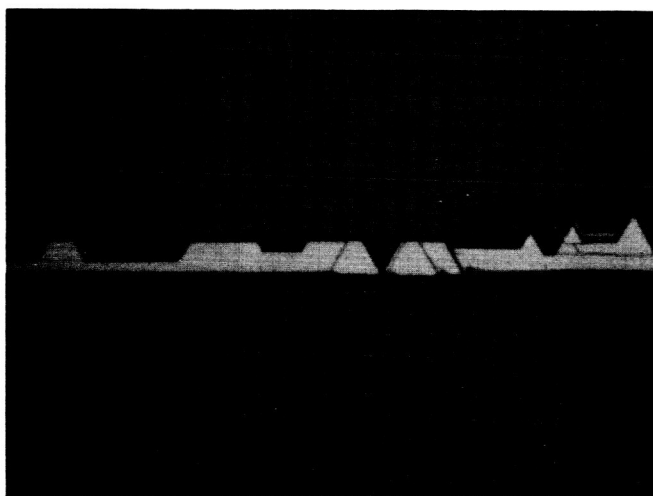
Layer line x-ray diffraction photographs were made of each of the whiskers. As previously mentioned, each proved to be of the a-type, i. e., the whisker axis was parallel to the a axis, $\langle h00 \rangle$, of the hexagonal unit cell of B_4C . In no case of the thermally treated whiskers was evidence of crystalline B_2O_3 found in the resulting x-ray diffraction pattern. This is not to say that B_2O_3 was not present. Rather, if present, it was not of high enough concentration (ca. 1 volume percent) to be detected by this x-ray method. Future work will be done using electron diffraction techniques which are suitable for the detection of thin crystalline surface films. Then too, it is possible that the B_2O_3 if present, is of a very small crystallite size and/or is non-crystalline making its detection by diffraction methods very difficult. It is suspected that the later postulation is perhaps true since the thermally treated (in air) specimen number 007 was found to contain glassy bulges along its entire length. This whisker produced a "clean" a-type B_4C diffraction photograph--without any indication of a second phase being present.

X-ray diffraction studies of B_4C whiskers have shown that in the "as-grown" condition clean shiny filaments of the variety employed in this study, are generally: (a) single crystals and (b) of the a-type. Interestingly however, specimens numbered 2, 4, 8, 10, 007 in Table II produced diffraction patterns which showed a degree of polycrystallinity (multiple spots).

To further elucidate the observations that a change in chemical behavior occurs at temperatures between 1000 and 1200°C, presumably, because of atmosphere attack, the following experiments were performed.



A.



B.

100 μ

Figure 12. Typical Surface Configurations Observed on B_4C Whiskers
(Magnification = 200X)

B_4C whiskers heated in air (at one atmosphere) to $1300^{\circ}C$ for 15 minutes were completely consumed which confirmed the severity of attack of B_4C by oxygen at these temperatures. By comparison, other B_4C whiskers heated to $1500^{\circ} - 1620^{\circ}C$ in vacuum were not consumed, but showed some surface alteration. Figure 13 is an optical micrograph (magnification - 429X) of a typical B_4C whisker which had received the vacuum heat treatment. It can be seen that the usual sharp cornered growth steps have been rounded off by the annealing treatments. B_4C whiskers heated in argon (one atmosphere) to $1300^{\circ}C$ for 15 minutes, also showed growth steps rounded off. In addition, what appears to be a second phase was observed on the surface of the whiskers treated in argon. Figure 14 is an optical micrograph (magnification - 429X) of one of these B_4C whisker. It is suspected that this surface debris is actually B_2O_3 droplets since the material has a glassy appearance. Further work will have to be done to further elucidate this observation.

It thus appears that B_4C whiskers are altered by heating to temperatures above $1000^{\circ}C$ in vacuum or argon. Part of this alteration could possibly result from a reaction between the B_4C whiskers and some component of the furnace atmosphere, such as residual oxygen or other oxidizing media. However, it is also very possible that the alterations arise because of enhanced evaporation at surface imperfections (areas of higher-than-average surface energy). Sears and DeVries⁽⁹⁾ have observed that surface imperfections in alumina whiskers can be annealed out and attribute their results to just such a mechanism.

It is possible then, that prolonged annealing of B_4C whiskers which contain surface imperfections can lead to an overall decrease in the number of imperfections and to an increase in the average strength. Such a technique could possibly upgrade the B_4C whiskers now being grown and therefore introduce a fruitful area for future study.

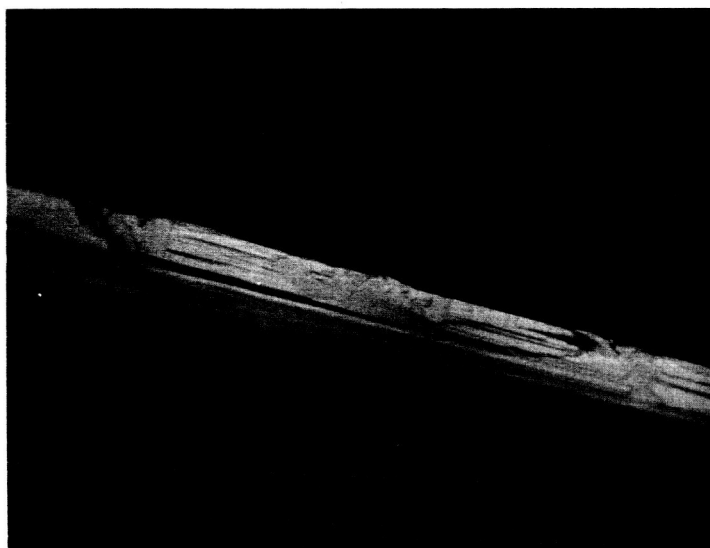


Figure 13. B₄C Whisker Photomicrograph at 429X After Vacuum Heat Treatment at 1550°C.

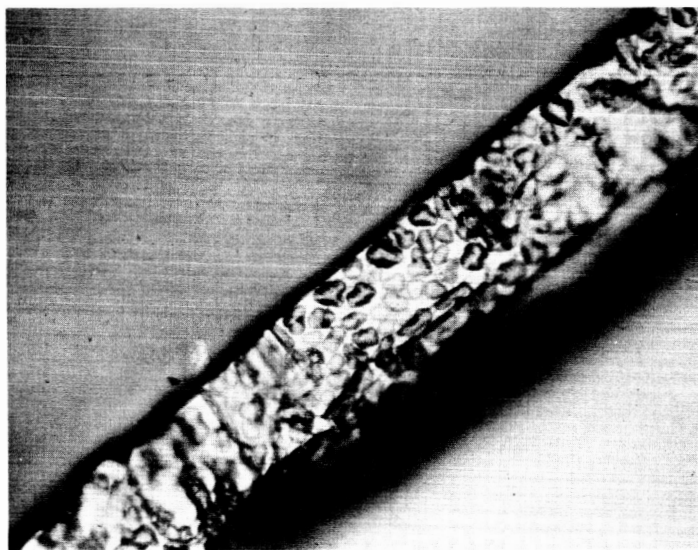


Figure 14. B_4C Whisker Photomicrograph at 429X After Argon Heat Treatment at $1300^{\circ}C$ for 15 Minutes.

IV. COMPOSITE STUDIES

Composite fabrication studies during this contract were performed utilizing conventional and modified hot pressing techniques and infiltration techniques.

A. SPECIMEN PREPARATION AND FABRICATION FOR HOT PRESSING TECHNIQUES

Conventional hot pressing was done in a steel heat-resistant die* capable of operating at temperatures as high as 600°C for extended periods. Its unique design minimizes and simplifies the number of parts necessary to function and also requires only punch changes and one half-a-die change in order to shift from one specimen cross-section to another. Thus, specimens can be fabricated with cross-sections varying from 1/8" x 1" to 1/16" x 1" with a minimum of shop time expended. Figure 15 is a photograph at about 1/2 size of a typical die which utilizes a 1/8" x 1" punch cross section. The modified hot pressing was performed in "Speer" graphite dies of the same design as the steel die of Figure 15.

Composite test specimens were prepared by several techniques and are discussed in the following paragraphs. Much of the effort was directed towards developing a procedure which would yield composites of B₄C whiskers in intimate contact with the aluminum matrix, but at the same time, which would not severely degrade or fracture the whiskers.

B. HOT-PRESSING METHODS

1. Conventional Hot-Pressing

A given quantity of B₄C whiskers was weighed out and mixed with -100 mesh Al powder so that the final volume percent of whiskers was 20%. The resulting mixture was then put into a graphite die and hot pressed to 2000 psi at 600°C. The specimens using this simple direct approach were not of good quality. Good mixing of the two phases was not possible because of density, size and shape differences. Also, during subsequent fabrication, the bridging and overlapping often resulted in excessive whisker breakage. This led to cracked and non-densified composite specimens.

*Peerless "A"

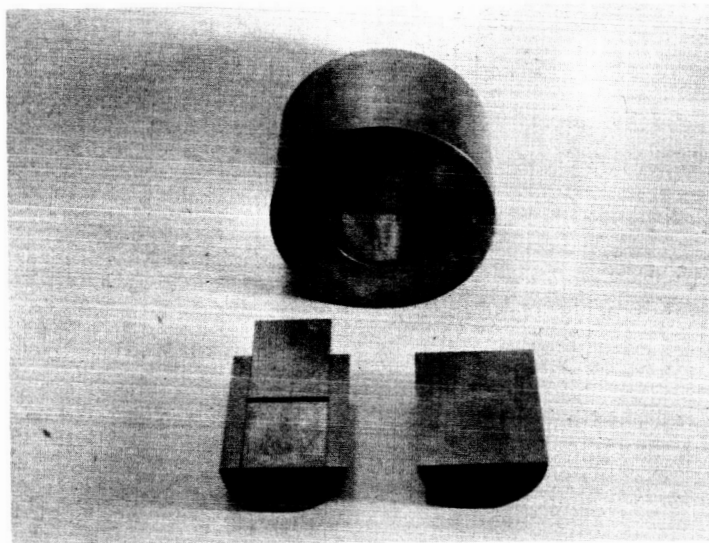


Figure 15. Steel Die Used to Hot Press Aluminum - B_4C Whisker Composites - About 1/2 Size.

2. Sandwich Method

Improved specimens were prepared by a modification which can be best described as a sandwich technique. The same basic technique was used maintaining the same weight of whiskers and aluminum powder; but in addition, a layer of aluminum powder was placed on the top and bottom of the composite mixture which eliminated direct die contact on the whiskers. A composite test specimen was easily prepared by filing away the excess aluminum left by the sandwiched structure. Excess aluminum was left on the ends of the specimens since it made an ideal gripping surface for tensile grips. A Schematic diagram of the fabrication sequence is shown in Figure 16. The whisker breaking problem was thus reduced considerably, but because of individual whisker to whisker contact, breakage was not eliminated.

3. Liquid Matrix Pressing Method

Another technique for forming Al-B₄C whisker composites utilized flake aluminum in conjunction with -100 mesh atomized aluminum. A slurry of B₄C whiskers and flake* aluminum was made using acetone as a dispersing medium. The Al flake size was such that wetting of individual B₄C whiskers by the slurry could be easily accomplished. The mixture was then dried and a sandwich formed and hot pressed. A typical microstructure of a B₄C-aluminum composite formed by this technique is shown in Figure 17.

Preliminary hot pressing studies were performed in graphite dies at temperatures below 660°C (m.p. of Al), at pressures not exceeding 4,000 psi. However, these conditions did not produce dense specimens in reasonable times. The pressing schedule was then revised so that the die temperature was allowed to reach 700°C. This temperature was sufficient to melt the aluminum metal of the composite sandwich, and also resulted in the extrusion of excess liquid metal out of the die. Because excess metal is added to a composite and can be ultimately squeezed out, the resulting composite can contain a high volume fraction of whiskers.

C. LIQUID INFILTRATION TECHNIQUES

In previous liquid infiltration experiments, difficulties were encountered because of the reaction between the molten aluminum and the fused silica molds which were used to contain the whiskers. This reaction limited the impregnation time which could be tolerated for a given infiltration run. Consequently, the time factor necessary for (1) the removal of absorbed gases or films originally present on the whisker surfaces, and (2) for the surface reaction between aluminum and the B₄C whiskers necessary for complete wetting was seldom achieved. As a result, the composites normally contained large voids and areas of poor fiber-matrix bonding.

*Pigment grade, flake size .1μ thick x 20μ x 200μ .

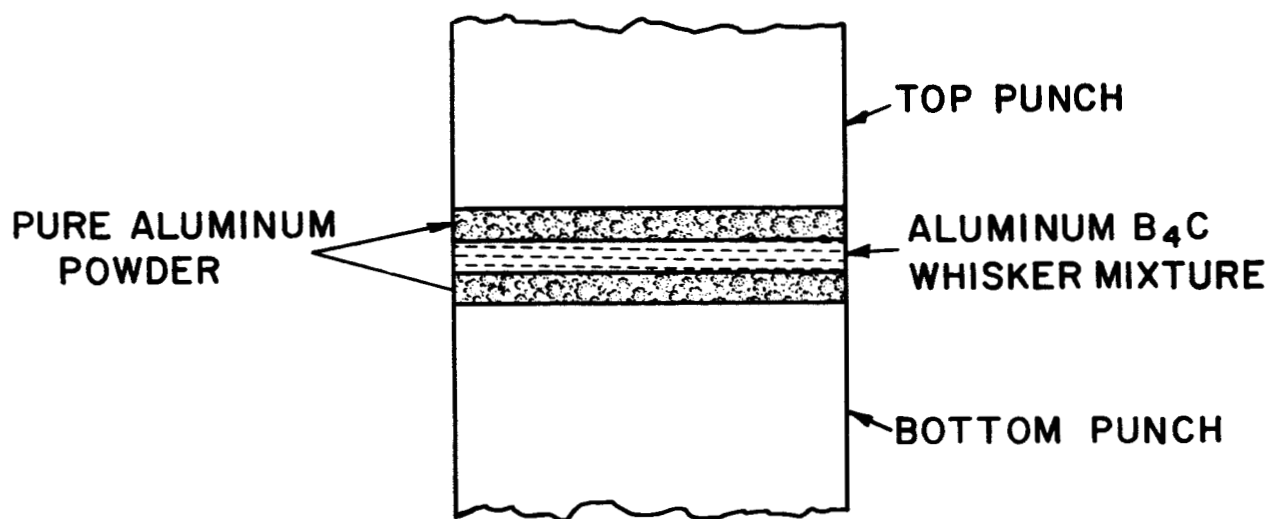


Figure 16. Schematic Diagram of Fabrication Sequence Followed to Produce "Sandwich" Specimen.

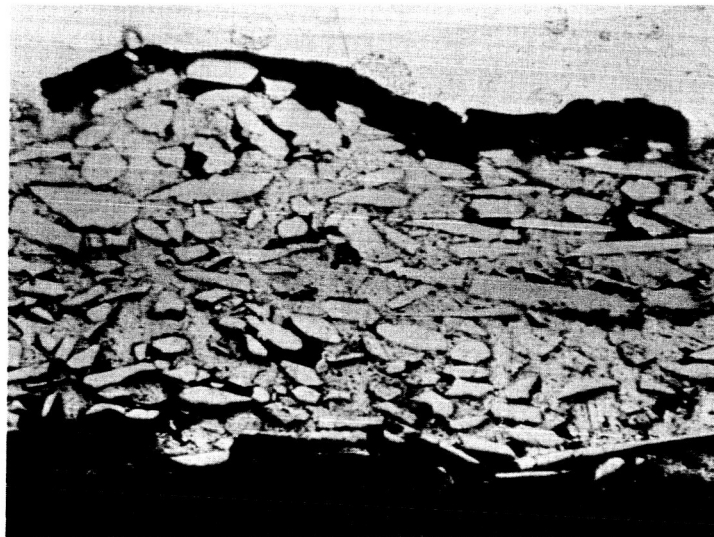


Figure 17. Typical Microstructure at 75X formed by "Sandwich" Technique in Conjunction with Aluminum Flake-B₄C Wisker Slurry.

Recently, new infiltration techniques have been developed under a separate contract ⁽¹⁰⁾ for forming composites of Al_2O_3 whiskers embedded in an aluminum matrix. These newly developed methods have eliminated the major problems previously encountered and are directly applicable to B_4C whisker-aluminum composites.

Hence, the experimental composite work was concentrated on applying the experience gained on recent related studies to the fabrication of aluminum- B_4C whisker composites by vacuum/pressure infiltration techniques.

The details of these investigations are summarized as follows:

1. Experimental Procedure

The apparatus and techniques utilized to fabricate the aluminum- B_4C whisker composites were basically the same as those described in detail by Mehan ⁽¹⁰⁾ for the fabrication of Al- Al_2O_3 composites. Briefly, the method consists of packing the whiskers to be infiltrated into the graphite mold section of an infiltration assembly shown in Figure 18. The infiltration assembly (consisting of the mold and a pneumatic pressurizing system) is positioned inside a vacuum chamber where the mold and crucible sections are heated by R. F. heating. When the proper conditions of temperature and atmosphere are achieved, the molten matrix metal is injected into the whisker bundle by pneumatic pressure.

Owing to the size and geometry of the B_4C whiskers grown to date, packing and orientation of the whiskers prior to composite fabrication was a major problem. The effectiveness of previously used orientation techniques was hampered by the short fiber lengths (ca. 2-5 mm) relative to the dimensions of the composites to be fabricated. Furthermore, the curved and kinked nature of the B_4C whiskers described in a previous section precluded packing to high volume fractions by techniques which would not cause appreciable breakage of the whiskers. The best results were obtained by funneling the B_4C whiskers into the mold cavity under vibratory action. Aluminum composite specimens were fabricated using both metal-coated and uncoated B_4C whiskers, and these will be described.

2. Fabricating Composites with Uncoated B_4C Whiskers

The initial experiments were conducted with uncoated B_4C whiskers since previous studies ⁽⁶⁾ had indicated that molten aluminum appeared to wet B_4C whiskers under the proper conditions. The first mold design tried was the same as shown in Figure 18. This design has been successfully used to fabricate Al- Al_2O_3 whisker composite rods 1/8 inch in diameter and 2 inches in length ⁽¹⁰⁾. The unique feature of this design is that it allows a metered volume of molten metal to flow through the whisker bundle and the small relief opening at the end of the mold prior to solidification. This is useful in

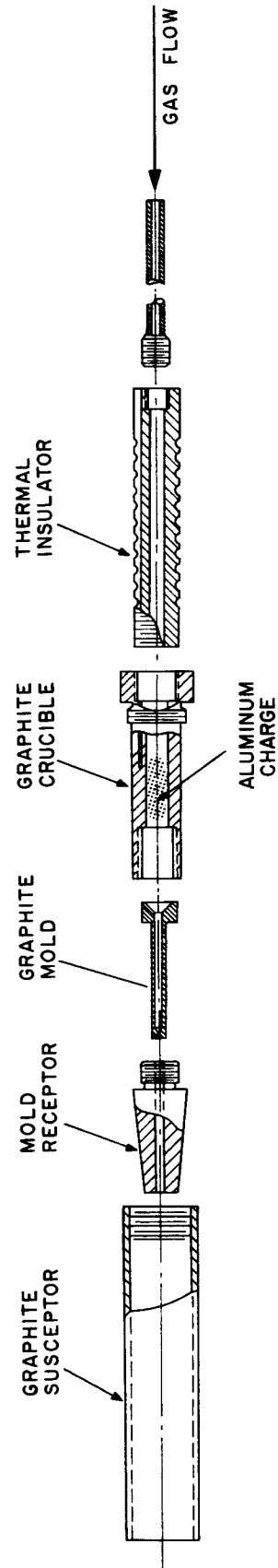


Figure 18. Infiltration Assembly

removing adsorbed gases from the mold and the fiber surfaces and enhances intimate contact between matrix and fiber.

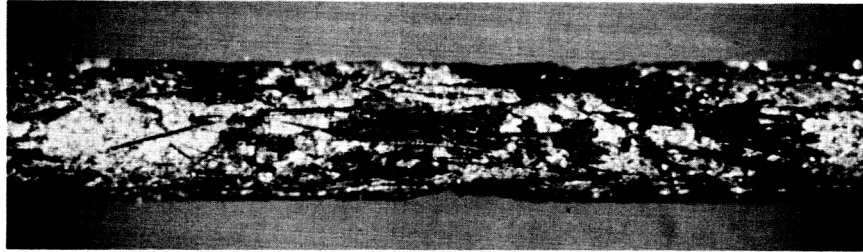
The results obtained with this method were discouraging. Although the metal would penetrate the B_4C whiskers, the whisker surfaces were apparently only partially wetted as indicated by the surface structure shown in Figure 19 A.

The next series of experiments was designed to allow for more prolonged contact between the molten metal and the B_4C whiskers under static (non-metal flow) conditions in order to increase surface reaction time and improve wetting. The procedure used was essentially the same as described above except that provisions were made for stopping the metal flow through the mold so that static contact between molten metal and fibers could be maintained. Residence times up to 4 minutes at $720^{\circ}C$ resulted in improved metal penetration as can be seen by comparing Figure 19 B with Figure 19 A. Longer residence times failed to produce further improvements. Despite the improved structures obtained, closer examination of the composite structures revealed that the wetting conditions had not yet been optimized. Therefore, the next experiments were conducted with B_4C whiskers which had been coated with a thin metal coating in order to promote wetting.

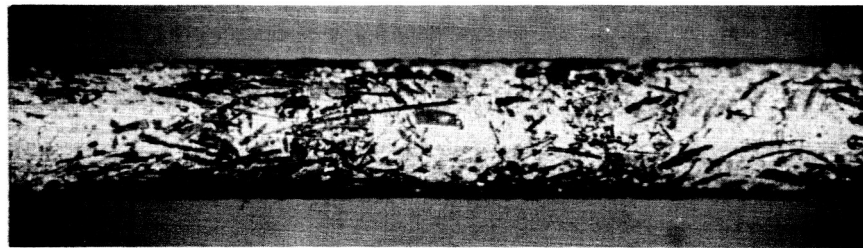
D. FABRICATING COMPOSITES WITH METALLIZED B_4C WHISKERS

Experience gained from past studies has indicated that surfaces metallized with a multi-layer consisting of a flash coating of titanium covered by a thicker ($\sim 0.5\mu$) coating of nickel are readily wet by molten aluminum. The high degree of wetting obtained with this system has been repeatedly demonstrated. Therefore, the B_4C whiskers were metallized with a Ti/Ni coating by techniques which have previously been described. The infiltration was accomplished in the same manner described above by allowing the molten metal to be in contact with the metallized B_4C whiskers for periods up to 4 minutes at $720^{\circ}C$ under static (non-flow) conditions. This method produced a notable improvement in the composite structures, as illustrated by the surface macrostructure of Figure 19 C. A typical composite cross-sectional microstructure is shown in Figure 20.

(A)



(B)



(C)

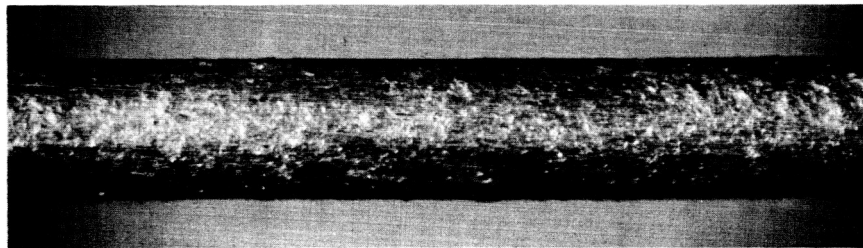


Figure 19 (A) Surface Features of an Aluminum Infiltrated Composite Using Uncoated B_4C Whiskers. (B) Surface of the same Type Composite as (A) Except for Longer Contact Time With Molten Aluminum. (C) Surface Features of an Aluminum Infiltrated Composite Containing Ni/Ti Coated B_4C Whiskers - 12X.

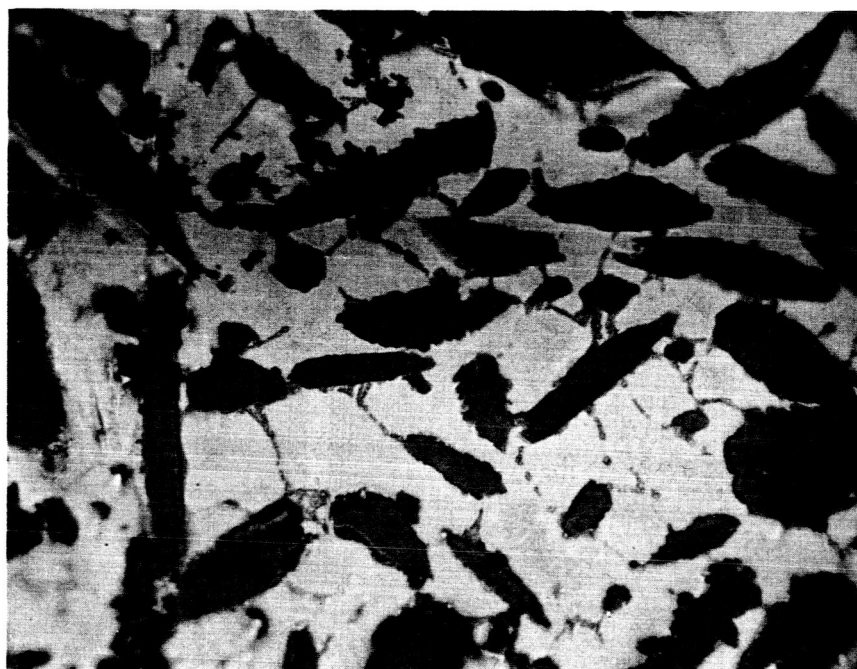


Figure 20. Cross-Section of the Microstructure
of a Composite Containing Ni/Ti
Coated Whiskers - 190X.

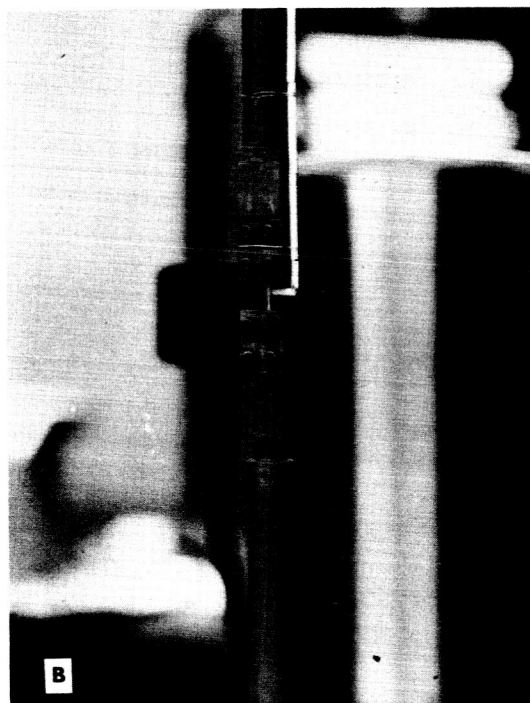
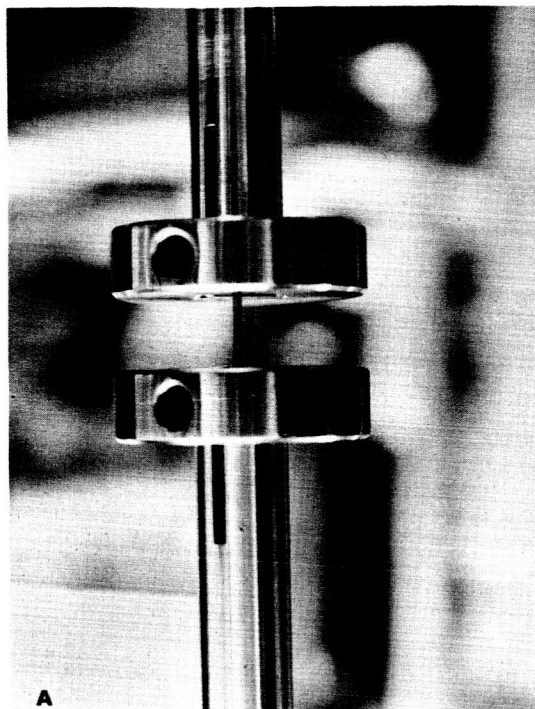


Figure 21. (A) Rigid Coupling System Used for Room Temperature Testing of B₄C-Aluminum Composites. (B) Flexible System for Elevated Temperature Testing of B₄C-Aluminum Composites.

3. Results and Discussion

The powder metallurgical techniques effectively combined the whiskers with the metal matrix. However, certain drawbacks of these processes should be noted, namely: (1) the volume fraction of whiskers in the resulting composites was limited, (2) the contact between all of the whisker surfaces and the metal matrix was poor, and (3) the whiskers were damaged mechanically. Thus, further infiltration experiments were made and excellent results were obtained. Although the whisker volume fractions achieved to date have been fairly low utilizing infiltration, the fiber orientation based on Figure 19 appears to be excellent. Furthermore, the results obtained are reproducible. It is anticipated that notable improvements in the whisker volume fractions and orientation will be made with continued improvements in the B_4C whisker growth products.

Tensile data derived from successful composites formed by both hot pressing techniques and infiltration techniques are summarized in Table III. Tests were conducted in an Instron Machine, utilizing a rigid coupling system at room temperature (Figure 21 A) and a flexible system for elevated temperature tests (Figure 21 B). These fixtures have been previously described⁽¹⁰⁾. The elevated temperature tests were performed in air using a standard nichrome wound tube furnace controlled by a chromel alumel thermocouple temperature sensing system.

The tensile values obtained at both room and elevated temperatures are about a factor of four greater than that expected for pure aluminum. Such behavior is to be expected since the volume fraction of B_4C whiskers contained in these composites averages about 5%. It is expected that as the quality (straightness and less tapers) of B_4C whiskers improves and as the techniques for sorting and packing whiskers improves, the volume fractions of strong B_4C whiskers will also greatly improve. These improvements in turn, should lead to composites of far greater strengths.

TABLE III. TENSILE DATA FOR B₄C-A1 COMPOSITES FORMED BY
HOT PRESSING AND INFILTRATION
TECHNIQUES

Sample #	Treatment	Test Temp. - °C	Ultimate Tensile Strength (psi)
BCC623016*	Hot Pressed-700 °C-15 min-2000 psi	RT	4,280
BC62365*	"	"	7,600
BC6230365*	"	"	3,666
BCC6240165*	"	"	20,500
BCC6240265*	"	"	14,750
BCC6250165+	"	"	16,000
BCC6250265+	"	"	14,300, 16,000
BC280165†	Hot Pressed-300 °C -5 min-24,000psi	"	2,600
BCC6290165+	Hot Pressed-480 °C-10 min-4,000psi	"	8,900
6021101	Infiltrated	RT	15,200
6021501	"	"	13,200
6021502	"	400	3,820
6021102	"	RT	13,200
6021503	"	250	8,150
6021104	"	410	4,100

*"V" Groove Sandwich

+ Sandwich

† Steel Jig

V. CONCLUSIONS

The best method utilized to date for growing B_4C whiskers has been the evaporation of B_4C powder at a temperature of about $1900^{\circ}C$ and then condensing the vapor at temperatures ranging between $185^{\circ}C$ to $1725^{\circ}C$ in the form of B_4C whiskers on a graphite substrate. Two furnace types were utilized; the first being a vertical tube furnace, where the powder was vaporized in a lower chamber and the vapor was allowed to condense on a graphite mandrel and chimney. However, this arrangement has resulted in whiskers having both a taper and curvature. The second furnace employs a centrally-heated horizontal tube of graphite containing the B_4C powder, which is vaporized and condensed on an outer, concentric cylinder of graphite. The use of this radial furnace resulted in straight B_4C whiskers growing in large numbers, although the whisker lengths were in general short. This furnace, however, offers the greatest potential in terms of both quality (high strength) and quantity of whisker product.

Another method for growing B_4C whiskers was investigated, which it was hoped, would yield large quantities of B_4C whiskers at lower temperatures. This procedure consisted of reacting solid B_2O_3 with carbon powder in an NH_3 atmosphere at $1400^{\circ}C$. However, in all of the experiments no whisker growth was observed, and the method was abandoned in favor of the pure vapor method using the radial furnace.

Calculations of the supersaturation coefficient, α , based on a theoretical model were made, and the results agreed very favorably with those derived from the experiments. A mechanism of B_4C whisker growth was also postulated.

Material characterization studies of growth anomalies which can occur under some B_4C whisker growth conditions has further extended the knowledge already gained in this field. As an example, long growth runs result not in longer, high quality whiskers but rather in whiskers that are coarse and contain polycrystalline surface deposits and dendritic growths. The polycrystalline deposits exhibit an orientation which is greatly influenced by the orientation of the supporting whisker (epitaxy).

Individual whiskers have been tested successfully, and information gained on characterization studies of these whiskers indicates that growth defects are a contributing factor to fracture of the whiskers at low load values. It is significant that a whisker which supported 2,000,00 psi was relatively free from growth defects, demonstrating the inherent strength capabilities of the perfect B_4C whisker.

B_4C whiskers tested at elevated temperature retained most of their strength at temperatures up to the $1000^{\circ}C$. However, at higher temperatures, the strength decreased rapidly; this decrease has been attributed to oxidation effects.

Annealing of B_4C whiskers in vacuum and argon at temperatures of $1300^{\circ}C$ to $1600^{\circ}C$ produces a modification of the imperfections (growth steps) on the surface of the whiskers. Such a mechanism can possibly upgrade the average strength of the as-grown whiskers.

Although no high strength composites have yet been fabricated, techniques have been developed which produce aluminum- B_4C composites of theoretical density by both hot pressing and infiltration techniques. Experience gained during this contract has contributed toward a better understanding of the problems associated with composite fabrication and have established important guidelines for producing improved composite specimens.

REFERENCES

1. A. Gatti, et al, "Synthesis of B_4C Filaments," NASw-670, Final Report July 10, 1964.
2. W. W. Pultz, "Method of Making Beta-Silicon Carbide Fibers", U. S. Pat. No. 3, 161,473, Dec. 15, 1964.
3. G. W. Sears, "A Mechanism of Whisker Growth," Acta Metallurgica, Vol. 3, No. 4, pg. 367, July 1955.
4. Harry E. Dobson and Paul W. Gillis, "The High Temperature Vaporization Properties of Boron Carbide and the Heat of Sublimation of Boron", Journal of Phys. Chem. Vol. 68, No. 5, May 15, 1964.
5. R. H. Doremns et al, edit. "Growth and Perfection of Crystals", John Wiley 1958.
6. A. Gatti, et al, "Study of the Growth Parameters Involved in Synthesizing Boron Carbide Filaments NASA CR-251, July 1965.
7. D. M. Marsh, "Stress Concentrations at Steps on Crystal Surfaces and Their Role in Fracture". "Fracture of Solids, AIME 1963, pg. 119-142.
8. T. N. Nazarchuk and L. N. Mekhanoshina, "Oxidation of Boron Carbide," Soviet Powder Metallurgy and Metal Ceramics, March-April 1964.
9. G. W. Sears and DeVries - Unpublished Research
10. R. L. Mehan, et al "Evaluation of Sapphire Wool and Its Incorporation Into Composites of High Strength". 3rd Quarterly Report, AF Contract AF33(615)-1696, Feb. 15, 1966.
11. J. Chorne', et al. Final Report Bu Weps, Contract NOw 65-0176c "Development of Composite Structural Materials For High Temperature Applications".

ACKNOWLEDGEMENTS

Acknowledgement is made to Messrs. T. Harris, E. Sauer, J. Kitler and V. Cordua for their valuable assistance in the program. Special acknowledgement is made to R. L. Mehan who supervised the mechanical tests and contributed to this report by summarizing this work.

DISTRIBUTION LIST

- | | |
|---|-----------------------------------|
| 1. Department of the Navy
Bureau of Naval Weapons
Munitions Building
Washington 25, D.C. | Attn: Mr. John Wright |
| 2. Wright Air Development Div.
Nonmetallic Materials Lab
Wright-Patterson Air Force Base, Ohio | Attn: Mr. R. C. Tomashot |
| 3. Wright Air Development Div.
Wright-Patterson Air Force Base, Ohio | Attn: Commander WWRNRE-4 |
| 4. H. I. Thompson Fiberglas Co.
1733 Condoza Street
Los Angeles 7, California | |
| 5. Defense Material Center
Battelle Memorial Institute
505 King Avenue
Columbus, Ohio | |
| 6. Boeing Airplane Co.
Aerospace Div.
Seattle 24, Washington | Attn: Mr. P. H. Entz |
| 7. Cornell Aeronautical Lab., Inc.
P.O. Box 235
Buffalo 21, New York | |
| 8. Hughes Aircraft Co.
Culver City, California | Attn: Mr. L. E. Gates, Jr. |
| 9. Applied Materials Physics Div.
Langley Research Center
National Aeronautics and Space
Administration
Langley, Virginia | Attn: Messrs. O. Trout/P. Hill |
| 10. Naval Research Laboratory
Washington 25, D. C. | Attn: Mr. J. A. Kies
Code 6210 |
| 11. Thiokol Chemical Corp.
Reaction Motors Div.
Denville, New Jersey | Attn: Miss M. Becker
Librarian |

DISTRIBUTION LIST (Cont'd)

12. Prof. H. T. Corton
Dept. of Theoretical and Applied Mechanics
University of Illinois
Urbana, Illinois
13. Texaco Experiments, Inc. Attn: Mr. Claude Tally
Richmond, Virginia
14. Jet Propulsion Lab Attn: Dr. M. Leippold/
California Institute of Technology P. J. Schlichta
4800 Oak Grove Drive
Pasadena, California
15. Mr. P. A. Hessinger
National Beryllia Corp.
First & Haskell Avenue
Haskell, New Jersey
16. George Mandel, Chief, Library
National Aeronautics & Space Administration
Lewis Research Center
21000 Brookpark Road
Cleveland 35, Ohio
17. R. Anderson
National Aeronautics & Space Administration
Langley Research Center
Langley, Virginia
18. W. Micks/L. Kaechle
Rand Corp.
1700 Main Street
Santa Monica, California
19. NASA Attn: Jerome Teplitz
Washington, D. C. 20546 Technology Utilization Div.
20. Prof. R. Ford Pray
Syracuse University
Syracuse, New York
21. I. Perlmutter
Wright Air Development Div.
Wright-Patterson Air Force Base, Ohio

DISTRIBUTION LIST (Cont'd)

22. L. Hjelm
Wright Air Development Div.
Wright-Patterson Air Force Base, Ohio
23. G. Peterson, WWRCNC-1
Wright Air Development Div.
Wright-Patterson Air Force Base, Ohio
24. D. Schmidt, WWRCBC-2
Wright Air Development Div.
Wright-Patterson Air Force Base, Ohio
25. J. D. Walton, Jr.
Head - Ceramics Branch
Georgia Institute of Technology
Atlanta 13, Georgia
26. Stanford Research Institute
Menlo Park, California
Attn: F. A. Halden
Ceramics Research Section
27. Cornell University
College of Engineering
Ithaca, New York
Attn: E. Scala
28. Owens-Corning Fiberglass Corp.
806 Connecticut Avenue, N.W.
Washington 6, D. C.
Attn: R. J. Weaver
29. NASA
Washington, D. C. 20546
Attn: Office of General Counsel-
Patents
30. New England Materials Laboratory, Inc.
P.O. Box 128
35 Commercial Street
Medford 55, Mass.
31. Mr. George Darcy
Ordnance Materials Research Office
Watertown Arsenal
Watertown, Mass.

DISTRIBUTION LIST (Cont'd)

32. Chemical Propulsion Information Agency
The Johns Hopkins University
Applied Physics Laboratory
8621 Georgia Avenue
Silversprings, Maryland
33. Sandia Corporation
Livermore Laboratory
P.O. Box 969
Livermore, California
Attn: Mr. E. A. Paxton,
Technical Library
- 34-39. National Aeronautics and Space
Administration
Office of Advanced Research and Technology
1512 H St., N. W.
Washington 25, D. C.
Attn: James J. Gangler (RRM)
40. Mr. J. Harry Jackson
General Director
Metallurgical Research Division
Reynolds Metals Company
Fourth and Canal Streets
Richmond 19, Virginia
41. Dr. Robert L. Coble
Associated Professor of Ceramics
Department of Metallurgy
Massachusetts Institute of Technology
Cambridge 39, Massachusetts
42. Professor Frederick R. Eirich
Department of Chemistry
Polytechnic Institute of Brooklyn
333 Jay Street
Brooklyn 1, New York
43. Dr. George A. Hoffman
Aero-Astronautics Department
The RAND Corporation
1700 Main Street
Santa Monica, California

DISTRIBUTION LIST (Cont'd)

44. Mr. Morton Kushner
Chief, Dyna Soar Materials
and Processes Unit
Aero Space Division
The Boeing Company
P.O. Box 3707
Seattle 24, Washington
45. Mr. William H. Otto
Research Specialist
Research and Development Division
Narmco Industries, Inc.
3540 Aero Court
San Diego 23, California
46. Mr. Arthur D. Schwope
Director, Mechanical Research Division
Clevite Corporation
540 East 105th Street
Cleveland 8, Ohio
47. Mr. Bernard Goldberg
U.S. Army Materials Research Agency
Attn: OPT
Watertown Arsenal
Watertown 72, Massachusetts
48. Mr. T. F. Kearns
Bureau of Naval Weapons
Code RRMA-2
Department of the Navy
Washington 25, D. C.
49. Mr. Henry Perry
Aeronautical Materials Consultant
Nonmetallic Division
U.S. Naval Ordnance Laboratory
White Oak, Silver Spring, Md.
50. Mr. Herbert F. Schwartz
Chief, Plastics & Composites Branch
Directorate of Materials & Processes
Aeronautical Systems Division
Wright-Patterson Air Force Base, Ohio

DISTRIBUTION LIST (Cont'd)

51. Capt. A. M. Blamphin, USN(ret.)
Materials Advisory Board
1155 - 16th St., N.W.
Washington, D.C.
52. National Aeronautics and Space Administration Attn: Dr. Henry Frankel
Goddard Space Flight Center Code 623
Greenbelt, Maryland
- 53-54. NASA Attn: Technical Information
Washington, D. C. 20546 Group (Code ATSS-AC)
55. Jim Withers
General Technology, Inc.
Alexandria, Va.
56. Oak Ridge National Laboratory, Attn: T. F. Connolly
Research Materials Information Center
P.O. Box X, Oak Ridge, Tennessee,
37831
57. National Aeronautics and Space Administration
Technology Utilization Division, Code ATU
Washington, D.C. 20546
58. National Aeronautics and Space Administration
Headquarters Contracts Division, Code BCA
Washington, D.C. 20546
59. Scientific and Technical Information Facility (4)
P.O. Box 5700
Bethesda, Maryland 20014
60. Mr. J. J. Krochmal
AFML - MAMC
Wright-Patterson Air Force Base, Ohio
- 61-63. NASA Attn: Mr. R. Signorelli
Lewis Research Center Mr. J. Wheeton
21000 Brook Park Dr. P. Probst
Cleveland, Ohio 44135

DISTRIBUTION LIST (Cont'd)

64. Mr. E. Mathauser
Langley Research Center
Langley Station
Hampton, Virginia, 23365

65. Mr. N. Mayer
NASA Hdqtrs.
Washington, D. C., 20546

66. Dr. J. Mueller
Ceramic Engineering Dept.
University of Washington
Seattle, Washington

INTERNAL - VFTC

Ed Blum	M1309
A. C. Harrison (1 + tissue)	Bldg. 500
A. Gatti (30)	M9124